Water vapor absorption spectrum between 13300 and 13800 cm^{-1}

I.S. Tyryshkin, Yu.N. Ponomarev, A.D. Bykov, B.A. Voronin, O.V. Naumenko, V.N. Savel'ev, and L.N. Sinitsa

Institute of Atmospheric Optics, Siberian Branch of the Russian Academy of Sciences, Tomsk

Received July 23, 1999

Water vapor absorption spectra were recorded between 13300 and 13800 cm^{-1} using a laser spectrophotometer employing a long-base cell (30 m) and alexandrite laser. Spectrum width of the emitted radiation was less then 0.005 cm^{-1}; optical path was 1200 m. Measurements were conducted at 10 Torr and the room temperature. The laser radiation wavelength was determined using an evacuated interferometer with the accuracy higher than 0.001 cm^{-1}. Measurements were made for 44 lines giving an addition to the spectrum previously reported by Mandin, Chevillard, Camy-Peyret, and Flaud [J. Mol. Spectrosc. **116**, 167–190 (1986)]. Positions and intensities of spectral lines were determined by fit of the Voigt profile to the observed values.

Introduction

Investigation of weak lines in the water vapor absorption spectrum is of interest in view of solving atmospheric optics problems. In particular, such lines can noticeably increase the total atmospheric absorption in the near IR or visible region, and this additional absorption should be taken into account together with other factors, such as continuum absorption, absorption due to water dimers, etc.,[1–2] when evaluating the radiative balance of the atmosphere.

On the other hand, the spectrum in the short-wave region (from the near infrared to the visible) is considerably denser due to strong vibrational excitation and resonance intensity redistribution. Because of the intensity redistribution, sufficiently strong lines corresponding to transitions to highly excited bending states, such as $(0v0)$, $(1v0)$, or $(0v1)$, can be observed in the spectrum. For example, sufficiently intense lines of the (060)–(000) band are easily observed in the 1-μm region due to the specific HEL-resonance.[3] Note also that these resonances cause appearance of lines of the (070)–(000), (080)–(000), and even (0 10 0)–(000) bands in the spectrum.[4] Investigation of line parameters of such bands is of interest for constructing the theory of highly excited rovibrational states, as well as for studying the role of a strong centrifugal distortion effect in formation of molecular spectra.

In this paper the water vapor absorption spectrum is analyzed in the 0.73-μm region. A laser spectrophotometer[5,6] with a long base cell and well controlled parameters (pressure, temperature) was used for the measurements. Thus, the spectroscopic parameters for even weak absorption lines could be determined accurately enough. The narrow-band alexandrite laser providing for measurements in the 720–780 nm (12800–13880 cm^{-1}) region was used as a radiation source. Earlier the measurements in the adjacent 13200–16500 cm^{-1} region were carried out by Mandin, Chevillard, Camy-Peyret, and Flaud[7] with the Fourier transform spectrometer giving the resolution of 0.013 cm^{-1}.

Experiment

The functional scheme of the spectrophotometer is shown in Fig. 1. The radiation from alexandrite laser *1* (Ref. 5) is directed by the beamsplitters to wavemeter *2*, spectral width meter *3*, and reference photoreceiver *4*. Then it passes through the optical system of multipass gas cell (MGC) *5* (Ref. 6) and is directed to measuring photoreceiver *6*. Photoelements are used as photoreceivers. Signals from the photoelements are recorded by V4–17 pulse voltmeters *7* and *8* and then inputted into computer through signal-to-code converters *9* and *10*. Spektron IV commercial wavemeter *2* with four incorporated evacuated Fiseau interferometers of 0.005 to 40 mm long bases is used for rough measurement of the radiation wavelength.

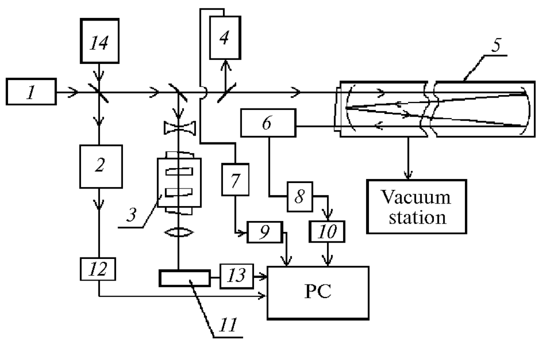

Fig. 1. Block diagram of the spectrometer.

Evacuated Fabri–Perot interferometer *3* with 80 mm base serves for more precise measurement of the wavelength and the spectrum width. The interference pattern at the interferometer output is recorded by the linear CCD array. Signals from the Spektron IV and the linear CCD array are inputted into PC through converters *12* and *13*.

0235-6880/99/09 792-04 $02.00

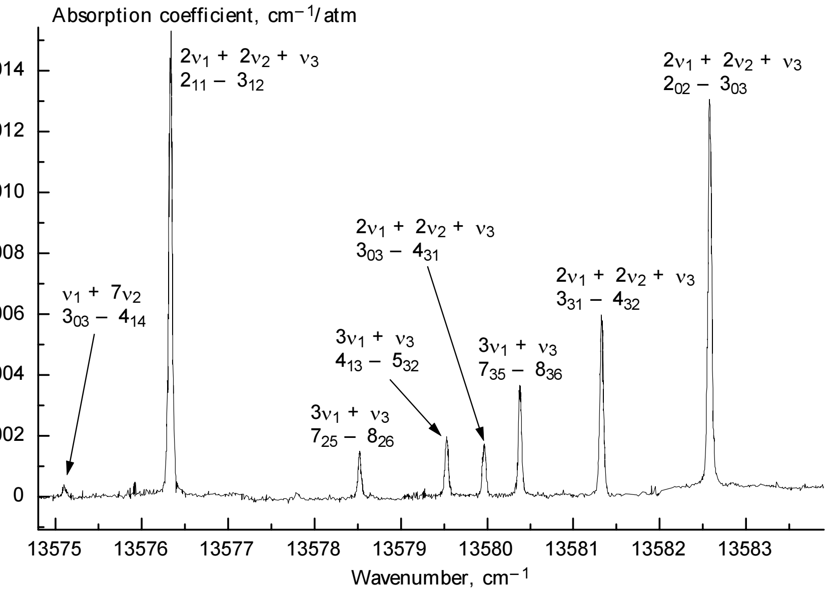

Fig. 2. Water vapor absorption spectrum in the 13575–13583 cm^{-1} region.

Specifications of the spectrophotometer

MGC:	
– length, m	30
– diameter, m	1.1
– pressure, Torr	$5\cdot10^{-5}$–10^3
– temperature, K	288–350
– optical path length, m	60–1800
Laser:	
– tuning range, nm	720–780
– spectrum width, cm^{-1}	$< 5\cdot10^{-3}$
– tuning step, cm^{-1}	$\ge 5\cdot10^{-3}$
– pulse repetition rate, Hz	≤ 10
– pulse duration, s	$\ge 180\ 10^{-9}$
– energy per pulse , J	$\ge 10^{-3}$
Recording system:	
– error in line positions, cm^{-1}	$\le 5\cdot10^{-3}$
– error in transmittance of the gas cell, %	≤ 1
– error in pressure, Torr	≤ 0.1
– threshold sensitivity, cm^{-1}	$5\cdot10^{-8}$

The transmittance of the analyzed gas is determined by the equation:

$$T_\lambda = (J_\lambda^{\rm out}/J_\lambda^{\rm in})/(J_{0\lambda}^{\rm out}/J_{0\lambda}^{\rm in}),$$

where the "in" and "out" superscripts correspond to the radiation intensity at the cell entrance and exit, respectively, while the "0" subscript denotes the values of the same parameters measured in the completely evacuated cell. The absorption coefficient is then determined from the measured transmittance T_λ using the Bouguer law.

A part of the spectrum is shown in Fig. 2 as an example. As is seen, the spectrum includes both strong ($2\nu_1 + 2\nu_2 + \nu_3$ band) and very weak ($\nu_1 + 7\nu_2$ band) lines. Note also a high signal-to-noise ratio. Examples of the spectrum records in the vicinity of some isolated absorption lines, as well as the results of Voigt profile fitting are shown in Figs. 3–5.

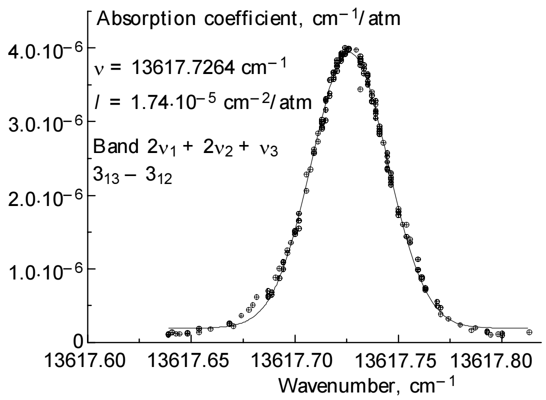

Fig. 3. Spectral dependence of the absorption coefficient for the 13617.7264 cm^{-1} line: measured values (circles), the result of Voigt profile fitting (solid curve).

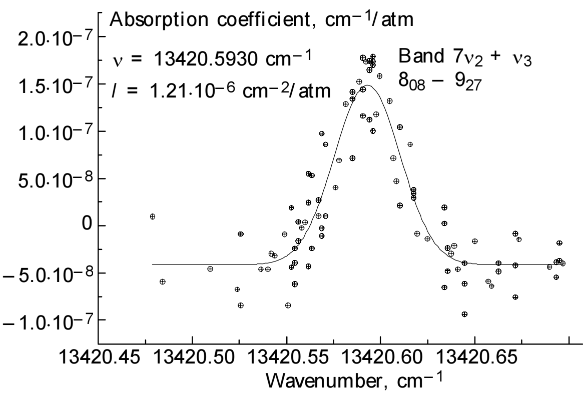

Fig. 4. Spectral dependence of the absorption coefficient for the 13420.5930 cm^{-1} line corresponding to the transition to the (071) highly excited bending state: measured values (circles), the result of Voigt profile fitting (solid curve).

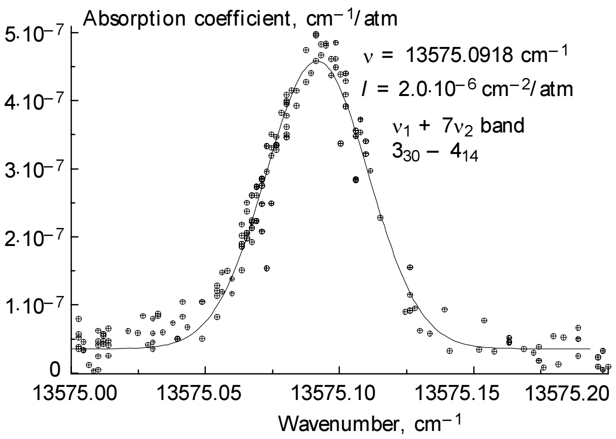

Fig. 5. Spectral dependence of the absorption coefficient for the 13575.0918 cm^{-1} line corresponding to the transition to the (170) highly excited bending state: measured values (circles), the result of Voigt profile fitting (solid curve).

Analysis and results

Lines were assigned on the basis of Partridge and Schwenke's *ab initio* calculations[8] of the positions and intensities of water vapor spectral lines. In addition to the results of Ref. 7, nine lines were assigned for the first time, and some lines were re-assigned (see also Ref. 9). Four lines formed by the transitions reaching the (160), (071), and (170) highly excited bending vibrational states were found in the spectrum.

The software developed by V.N. Savel'ev was used for processing the experiment and retrieving the positions and intensities of weak lines. It allows determination of the base line and least-square fitting of line positions, intensities, and halfwidths with the use of different line profiles. In this work the Voigt profile was used; the results of fitting are presented in Table 1. The first column of the table shows line positions with the 1σ confidential intervals given in parentheses in the units of least significant digits. Line intensities followed by their uncertainties are presented in the second and third columns. The ratio $R = I_f/I_n$ is given in the fourth column, where I_f denotes the intensities measured in this work, while I_n stands for the data from Ref. 7. Vibrational and rotational quantum numbers of the transitions are given in the last columns.

The comparison of the line centers obtained in this work with those of Ref. 7 shows their agreement within the experimental error for the most measured lines with the differences being, as a rule, several thousandths reciprocal centimeter. However, for some lines the differences are large enough, for example, for the line at 13445.4598 cm^{-1} the discrepancy exceeds 0.02 cm^{-1}. Since the measurements in Ref. 7 were conducted at lower spectral resolution (0.013 cm^{-1}), it seems reasonable to consider our value of the line position being more precise than that of Ref. 7 (13445.4613 cm^{-1}).

Table 1. H_2O spectral line positions and intensities in the 13300–13800 cm^{-1} region

Center, cm^{-1}	Intensity, cm^{-2}/atm	Δ	R	$v_1' v_2' v_3' - v_1 v_2 v_3$	$J' K_a' K_c'$	$J K_a K_c$
13331.3197(15)	4.123 10^{-7}	1.5 10^{-7}	–	(301)–(000)	7 3 5	8 5 4
13370.0437(4)	1.113 10^{-6}	1.4 10^{-7}	–	(221)–(000)	10 0 10	11 0 11
13420.5930(7)	1.207 10^{-6}	3.0 10^{-7}	–	(071)–(000)	8 2 6	9 2 7
13426.8801(6)	1.487 10^{-6}	3.3 10^{-7}	–	(221)–(000)	8 0 8	9 2 7
13445.4598(6)	1.245 10^{-6}	2.5 10^{-7}	–	(221)–(000)	7 2 5	8 2 6
13462.7748(1)	6.293 10^{-6}	2.1 10^{-7}	1.06	(221)–(000)	7 2 6	8 2 7
13565.7823(5)	3.099 10^{-6}	4.8 10^{-7}	–	(202)–(000)	4 3 2	5 4 1
13565.9669(2)	1.419 10^{-6}	1.1 10^{-7}	–	(221)–(000)	7 2 6	7 2 5
13566.2543(1)	1.084 10^{-4}	4.2 10^{-6}	0.66	(221)–(000)	3 1 3	4 1 4
13570.6758(5)	1.129 10^{-6}	2.9 10^{-7}	–	(301)–(000)	8 1 7	9 1 8
13571.0721(3)	7.141 10^{-6}	8.4 10^{-7}	1.23	(170)–(000)	9 0 9	10 1 10
13572.0969(8)	9.268 10^{-6}	2.8 10^{-6}	0.98	(202)–(000)	9 3 7	10 0 10
13572.6183(1)	2.590 10^{-5}	1.1 10^{-6}	–	(301)–(000)	9 1 9	10 1 10
13572.8144(2)	1.548 10^{-5}	1.3 10^{-6}	–	(221)–(000)	4 4 0	5 4 1
13573.4615(2)	2.005 10^{-5}	1.4 10^{-6}	1.03	(202)–(000)	8 2 7	9 1 8
13574.5466(6)	2.502 10^{-6}	5.2 10^{-7}	–	(202)–(000)	6 2 4	7 3 5
13575.0918(2)	2.003 10^{-6}	1.6 10^{-7}	–	(170)–(000)	3 0 3	4 1 4
13576.3323(1)	8.441 10^{-5}	4.5 10^{-6}	0.82	(221)–(000)	2 1 1	3 1 2
13578.5226(2)	7.385 10^{-6}	3.8 10^{-6}	–	(301)–(000)	7 2 5	8 2 6
13579.5312(2)	9.988 10^{-6}	6.1 10^{-7}	1.27	(301)–(000)	4 3 1	5 3 2
13579.9661(2)	9.820 10^{-6}	9.0 10^{-7}	1.12	(221)–(000)	3 3 0	4 3 1
13580.3691(1)	2.052 10^{-5}	7.2 10^{-7}	0.80	(301)–(000)	7 3 5	8 3 6
13581.3279(2)	3.503 10^{-5}	2.3 10^{-6}	0.86	(221)–(000)	3 3 1	4 3 2
13582.5794(1)	7.211 10^{-5}	3.9 10^{-7}	0.86	(221)–(000)	2 0 2	3 0 3
13606.2272(4)	8.607 10^{-7}	1.3 10^{-7}	–	(202)–(000)	9 3 7	9 2 8
13608.0885(3)	1.478 10^{-6}	1.4 10^{-7}	–	(301)–(000)	9 1 9	9 1 8
13617.7265(1)	1.744 10^{-5}	3.5 10^{-7}	1.06	(221)–(000)	3 1 3	3 1 2
13733.0701(4)	4.867 10^{-5}	9.8 10^{-6}	1.03	(221)–(000)	3 2 2	2 2 1

Table 1 (continued)

Center, cm^{-1}	Intensity, cm^{-2}/atm	Δ	R	$v_1' v_2' v_3' - v_1 v_2 v_3$	$J' K_a' K_c'$	$J K_a K_c$
13734.7908(1)	$4.119\ 10^{-5}$	$1.9\ 10^{-6}$	1.10	(301)–(000)	5 1 5	5 1 4
13735.6196(4)	$8.522\ 10^{-6}$	$1.3\ 10^{-6}$	–	(202)–(000)	5 2 3	5 3 2
13736.1203(1)	$1.683\ 10^{-4}$	$5.7\ 10^{-6}$	0.76	(301)–(000)	3 0 3	4 0 4
13737.0708(6)	$1.585\ 10^{-6}$	$6.2\ 10^{-7}$	–	(301)–(000)	3 1 3	4 1 4
13737.7425(3)	$2.494\ 10^{-5}$	$2.9\ 10^{-7}$	0.63	(221)–(000)	3 2 1	2 2 0
13737.9062(1)	$4.841\ 10^{-5}$	$2.2\ 10^{-6}$	1.05	(301)–(000)	4 0 4	4 2 3
13738.9965(1)	$1.044\ 10^{-4}$	$1.7\ 10^{-6}$	0.74	(221)–(000)	3 3 1	4 1 4
13739.4420(1)	$8.783\ 10^{-5}$	$1.9\ 10^{-6}$	1.05	(221)–(000)	5 1 5	4 1 4
13740.2548(3)	$1.110\ 10^{-5}$	$2.1\ 10^{-6}$	–	(301)–(000)	6 2 5	6 2 4
13740.3935(2)	$3.814\ 10^{-5}$	$3.5\ 10^{-6}$	–	(221)–(000)	5 0 5	4 0 4
13741.0750(9)	$1.843\ 10^{-5}$	$4.7\ 10^{-6}$	–	(202)–(000)	3 2 2	4 1 3
13741.1530(8)	$2.139\ 10^{-4}$	$1.1\ 10^{-5}$	1.38	(301)–(000)	2 2 0	3 2 1
13768.9039(1)	$8.857\ 10^{-5}$	$2.5\ 10^{-6}$	–	(301)–(000)	5 2 4	5 2 3
13768,9743(1)	$4.387\ 10^{-5}$	$2.1\ 10^{-6}$	–	(301)–(000)	6 2 4	6 4 3
13796.7772(14)	$3.387\ 10^{-7}$	$4.0\ 10^{-7}$	–	(122)–(000)	4 0 4	5 1 5
13796.8667(1)	$1.052\ 10^{-5}$	$5.9\ 10^{-7}$	–	(160)–(000)	7 5 2	6 2 5

The comparison of the line intensities obtained in this work with those given in Ref. 7 (for 20 lines) shows close agreement mostly within the total measurement error. The ratio R, on average, is 1.025±0.20 with the maximum deviation of 40% observed for the line at 13737.7425 cm^{-1}.

The intensities of transitions reaching the high (160), (170), and (071) states prove to be as large as 10^{-5} cm^{-2}/atm. This is explained by the resonance intensity redistribution from the strong line-partners of the (301)–(000) and (221)–(000) bands.

Acknowledgments

Authors are grateful to Corresponding Member of the Russian Academy of Sciences, Professor S.D. Tvorogov for his interest to this work.

This work was supported in part by the President of the Russian Federation, Grant No. 96–15–98476/School and by the Russian Foundation for Basic Research, Grant No. 99–03–33210.

References

1. A.D. Bykov, B.A. Voronin, O.V. Naumenko, L.N. Sinitsa, K.M. Firsov, and T.Yu. Chesnokova, Atmos. Oceanic Opt. **12**, No. 9, 787–789 (1999).
2. R.C.M. Lerner, "*The capacity of atmosphere. An estimate of the contribution due to unknown, weak absorption lines in the water spectrum*,B*Report on Water Conference*, Paris (1998).
3. A.D. Bykov, O.V. Naumenko, and L.N. Sinitsa, Atm. Opt. **3**, 1014–1018 (1990).
4. C. Camy-Peyret, J.-M. Flaud, A.D. Bykov, et al, in: *Proceedings of the XIII Symposium on High Resolution Molecular Spectroscopy HighRus'99* (Tomsk, 1999), p. 72.
5. I.S. Tyryshkin, N.A. Ivanov, and V.M. Khulugurov, Kvant. Elektron. **25**, No. 6 , 505 (1998).
6. Yu.N. Ponomarev and I.S. Tyryshkin, in: *Regional Monitoring of the Atmosphere.* Part 3. *Unique Measuring Systems*, ed. by M.V. Kabanov (Novosibirsk, 1998), 287 pp.
7. J.-Y. Mandin, J.-P. Chevillard, C. Camy-Peyret, and J. M. Flaud, J. Mol. Spectrosc. **116**, 167–190 (1986).
8. H. Partridge and D.W. Schwenke, J. Chem. Phys. **106**, 4618–4639 (1997).
9. O.L. Polyansky, N.F. Zobov, S. Viti, and J. Tennyson, J. Mol. Spectrosc. **189**, 291–300 (1998).